# Preliminary Study on Analytical Prediction Model of Local Impact Phenomena on Concrete Structures against Hard Missiles

Qadir Bux alias Imran Latif, Ahmad Mujahid Ahmad Zaidi and Ismail Abdul Rahman

*Abstract*-Concrete is basic construction material used for many kind of structure. However, in the majority essential structures such as nuclear plants, Power plants, Weapon Industries, weapons storage places, water retaining structures like dams, & etc., concrete structures have to be designed as self-protective structure endow with defense against any disaster or consciously engendered unpleasant incidents such as terrorist attack, war, missile attacked by war jets, and dynamic loading, dynamic local impact damage and global damage generated by kinetic missiles. This study inquisitively is paying attention on verdict the numerical simulation on the behavior of concrete structures against local impact effect generated by hard missile. The fallout conquer from this study can be used for making design counsel and design procedures for seminal the dynamic retort of the target to foil local and global impact damage. This paper only endow with the appraisal of prior analytical model investigation connected with our study.

*Keywords*: local impact phenomena, hard missile, penetration, perforation, scabbing.

## I. INTRODUCTION

Over the years, concrete is very commonly used construction material for the defensive and civil applications to protect structures from local and explosive impact loads. For the designing of premium shielding structures it is vital to have a good knowledge about deeds of concrete against impact or explosive loading conditions. Projectile may be exists in a long diversity with fluctuation in sizes, shapes, velocity, weight, density, such as bullets, fragments, tornado, terrorist bombing, etc. The projectile may be classified as 'Hard' and 'Soft' depending upon deformability of projectile with respect to target's deformation. Deformation of hard missile is considerable smaller or negligible compared with target's deformation.

Qadir Bux alias Imran Latif is a Master student by research, Faculty of Civil & Enivirnomental Engineering, Universiti Tun Hussein Onn Malaysia, 86400 Parit Raja, batu Pahat, Johor Darul Ta'zim. (corresponding author to provide phone: +6019-7013878; e-mail: imranqazi37@gmail.com).

Dr. Ahmad Mujahid Ahmad Zaidi is a Lecturer, Faculty of Mechanical Engineering, Universiti Tun Hussein Onn Malaysia, 86400 Parit Raja, batu Pahat, Johor Darul Ta'zim. (corresponding author to provide phone: +6017-4783139; e-mail: mujahid@uthm.edu.my).

Dr. Hj. Ismail Abdul Rahman is a Deputy Dean, Faculty of Civil & Enivirnomental Engineering, Universiti Tun Hussein Onn Malaysia, 86400 Parit Raja, batu Pahat, Johor Darul Ta'zim. (corresponding author to provide phone: +6012-7876360; e-mail: ismailar@uthm.edu.my).

Almost in all cases hard missiles are considered as non – deformable or rigid. However, 'Soft' missile deforms itself considerably well as compared to target's deformation. Interest is focused on local damage and global response of target deformation caused by 'Hard' missiles considering failure criteria, contact mechanics, material model, and parametric analysis (velocity of missile, distance b/w missile and target, weight of missile, size and shape of missile, angle at which missile attacks on target, density of missile and target, thickness of structure, strength of concrete and reinforcement of concrete). Local impact effect consists mainly four process: (i) Spalling of concrete (ejection of material from front face or impacted face), (ii) scabbing of concrete (peeling off of material from back face or opposite side of impacted face of target), (iii) Missile Penetration into target (displacement of missile into the target), and (iv) Perforation of the target (full penetration beyond target). The local impact effect of hard missile on concrete structures can be studied by three ways, (i). Empirical Studies (predict empirical formula based on experimental data), (ii). Analytical Studies (create formula based on physical laws and compared with experimental data), and (iii), Numerical Simulation (based on computer based material model generate results and compared with experimental data). This study is based on numerical simulation with the help of finite elements.

*Local Phenomena:* There're two assortments of impact occurs at target, when it is subjected to projectile. First one is local impact and other one is explosive impact. The damage caused by projectile with its physical parameters, not because of explosion is known as local impact damage. Local impact effect is further briefly sub-divided in below explained processes:

- Radial cracking,
- Spalling,
- Penetration,
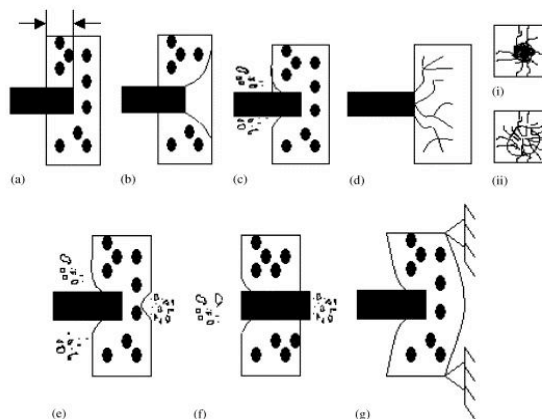- Cone cracking and plugging,
- Scabbing, and
- Perforation.

Fig.1. Explains the local impact phenomena caused by hard projectile. (a) Penetration, (b) Cone cracking and Plugging, (c) Spalling, (d) Radial cracking, (e) Scabbing, (f) Perforation, and (g) Global phenomena.

**Radial Cracking:** When projectile thump the target with very low velocities, in the result projectile become rebound without producing any local damage to target only just produced hair cracks on impacted area. The increase in velocity causes local damage on the impacted surface of target, the impact generates increase in hair cracks and figure radial cracks originated from the point of impact within the target in every direction.

**Spalling:** The increase in velocity cause more impact, it cause ejection of material of target from front face (impacted face). Due to impact of hard projectile, spalling produces spall crater in the surrounding area of impact. Spall crater is the total damaged portion of peeling off material from target on impacted face.

**Penetration:** penetration is defined as the infiltration or digging of missile into the target body afar from the thickness of spall crater. The lengthwise measurement of dig is called penetration depth. Penetration further can be explained as when the missile goes through in a semi-infinite medium of target, it causes no effect on rear face.

**Cone cracking & Plugging:** During penetration missile with plastic shocks having larger vigor than the elastic waves colloids with rear border of target and generates curved shear cracks in the shape of bell plug is called cone cracking. And than missile continues penetrating through target, it forces plug and shears-off the surrounding material of target is called plugging. This process generates rapid change into the behavior of target.

**Scabbing:** Scabbing occurs when the dynamic force in shape of waves generated by projectile within the target become equal or greater than the tensile strength of target. Generally scabbing occurs after plugging process. Ejection of target material from back face of target is called scabbing.

**Perforation:** The last process of damage due to hard missile impact is perforation. Perforation means complete passage or complete crossing of projectile through the target. It causes missile to extend penetration hole through scabbing crater and exit from the rear face of target.

## II. REVIEW OF ANALYTICAL STUDIES ON LOCAL IMPACT EFFECTS OF HARD PROJECTILE ON CONCRETE STRUCTURE

**Analytical models for Penetration depth (x):** The prime issue in an analytical penetration model is to correct formulation of the resultant penetration resistance force ($F_R$), offered by concrete target on the projectile during penetration. The Newton's second law of motion ruled the linear motion of the rigid projectile:

$$M(dV/dt) = -F_R, \tag{1}$$

With initial conditions $V = V_o$ at $t = 0$, and $X = 0$ at $t = 0$, where $V = (dX/dt)$, $X$ and $V$ are the instantaneous penetration depth and projectile velocity respectively. The above eq. # 1: controls the motion of projectile and penetration depth.

The penetration resistance formulated as function of the projectile velocity to include the dynamic effects in a penetration process.

Often, the penetration resistance force takes the form of binomial function of the instantaneous projectile velocity [4, 5],

$$F_R = F_R(V) = A_1 + A_2V + A_3V^2 + \ldots\ldots, \tag{2}$$

Where $A_1$, $A_2$, and $A_3$ can be considered as approximate constant parameters determined by the geometry of projectile nose and the mechanical properties of the target. Forrestal et al. suggested in [6] experimental determination of function $F_R(V)$ in above equation is possible from deceleration-time data in instrumented penetration tests. In [6] he also mentioned that a two-term penetration resistance ($A_2 = 0$ in above Eq.) gave excellent agreement with instrumented experimental results, however, it underestimated the experimental results for a 39MPa concrete target when the CRH of the projectile becomes large.

In eighteenth to nineteenth centuries in the early work of Robins and Euler took $A_1$ and $A_2$ equal to zero, which was further developed by Allen et al. [4] to relate the coefficient of the penetration resistance for sand to the drag coefficient as in aerodynamics.

$$F_R = (1/2) C_d \ A V^2, \tag{3}$$

Where $A$, are the presentation area on a plane normal to the flight line, and density of the medium respectively, and $C_d$ is drag co-efficient, for granular medium $C_d$ can be considered as constant over wide velocity range, although for more accuracy it should be formulated as function of the projectile velocity.

Poncelet (1788 – 1867) suggested a more realistic expression for the resistance force function:

$$F_R = A (a + bV^2) \tag{4}$$

Where A is the cross-sectional area of the projectile nose it equals to $A_0$ when the projectile nose is completely embedded into the concrete target, where $A_0$ is the cross-sectional area of the projectile shank), and a and b are constants can be determined by the geometry of the projectile nose and the mechanical properties of target. Poncelet formula further illustrated through dynamic cavity expansion theory. Wen [7, 8] suggested a linear expression of penetration resistance force:

$$F_R = A [ \ f_c + \ V \ ( \ f_c)^{1/2}], \tag{5}$$

Where $f_c$ is quasi-static target material strength, and are constants that are determined either experimentally or theoretically. Values of , and $f_c$ were recommended for four common nose shapes for various target materials and reasonable agreement between predictions and experimental data were obtained for a collection of penetration and perforation tests [7,8].

Dynamic cavity expansion theory offers a theoretical foundation for the Poncelet resistance function. The pioneer work of Bishop et al. [9] employed quasi-static equations for the expansion of cylindrical and spherical cavities to estimate the resistance force applied on the conical nose when it punches slowly into a metal target. Hill [10] and Hopkins [11] developed the dynamic cavity expansion equations for an incompressible target material, which was applied by Goodier [12], including target inertia effects, to predict the penetration depth of a rigid sphere into metal targets.

In the last decade, the dynamic cavity expansion theory vastly used for the study of deep penetration of projectiles in to metal, concrete and soil targets [13, 14, 15, 16, 17, and 18]. Li and Chen [15] further modified the Forrestal's concrete target penetration model [13, 16] to projectile having general nose shapes and two independent non – dimensional parameters were introduced to determine the penetration depth (x). The axial resistance force on the projectile nose, when the interface friction between the projectile nose and concrete target is neglected:

$$F_R = cx \qquad \text{for } x < kd \qquad (6)$$

During spall cratering, and during penetration:

$$Fr = \frac{\pi d^2}{4}\left(Sf_c + N^*\ell V^2\right) \qquad \text{for } x \geq kd \qquad (7)$$

Where c can be calculated:

$$c = \frac{\pi d}{4k}\frac{\left(N^*\ell V_o^2 + Sf_c\right)}{\left(1 + \left(\pi kd^3/4M\right)N^*\ell\right)} \qquad (8)$$

S, k and N can be calculated by using semi analytical formulae given in previous section.

The dynamic cavity expansion theory further modified to accommodate different material characteristics. Xu et al. [20] developed an elastic-cracking resistance force model based on the dynamic spherical cavity expansion theory when considering the post – test observations that concrete cracks in the region surrounding the projectile. Durban and Masri [21] studied the dynamic cavity expansion theory in pressure – sensitive elastoplastic media based on the Druucker – Prager plasticity model, which has been used as constitutive equation for describing the non – elastic deformation the range of geo – materials and concrete.

In addition the projectile velocity and penetration depth is also considered in the formulation of the penetration resistance function,

$$F_R = F_R (V,x). \qquad (9)$$

Murff and Coyle [22] introduced a polynomial function of x and V for penetration into clay:

$$F_R = A_1 + A_2x + A_3x^2 + A_4V + A_5Vx + \ldots, \qquad (10)$$

Where co – efficient $A_i$ can be determined from experimental data for variety of projectiles nose length, diameter, and impact velocity.

An approximate penetration theory was established based on impact force time history, which can be represented by Separable force law, that theory engaged in the establishment of the modified NDRC formula [1, 23], viz.

$$F_R = g(x/d) \, f(v), \qquad (11)$$

Where g – function is non – dimensional and given as:

$$g(x/d) = \begin{cases} x/2d & \text{for } x/d \leq 2 \\ 1 & \text{for } x/d > 2 \end{cases} \qquad (12)$$

And

$$f(v) = \frac{1466\sqrt{f_c}}{N^*}\left(V/12000d\right)^{.2} \qquad (13)$$

where n is nose shape factor defined already in modified NDRC formulae, Riera [24] suggested a – function, for normal penetration distance. The resistance function is independent of V, f(V) = 1, and

$$g(x/d) = \frac{\pi d^2 f_c \beta}{4}\frac{x}{d} \qquad (14)$$

Where

$$\beta(x/d) = \beta_1 - \beta_2 \exp(-cx/d)/N^* \qquad (15)$$

Where N is the nose shape factor introduced in the modified NDRC formulae, the penetration formula was given in terms of the impact factor introduced in [25] and $_1$, $_2$, c were obtained through regression method by fitting experimental data on penetration depth:

$$I_a = 194.59(x/d) - 322.27\left[1 - \exp\left(-0.598\frac{x}{d}\right)\right] \qquad (16)$$

In early 1970s The AVCO Corporation was proposed an analytical method to provide explicit formulations for the normal and tangential stresses on the projectile based on rigid projectile assumption, by using differential area force law (DAFL)" [26]. They produce this formula in cooperation with six independent linear and momentum equations for rigid body and their respective initial conditions, control the dynamics of a projectile during penetration. Later on the US Army Waterways Experiment Station (WES) modified the DAFL approach to make available 2D (PENCO2D) and 3D (PENCRV3D) codes for projectile trajectory analyses [27 – 29].

In the end, Sandia National Lab has combined dynamic cavity expansion theory with finite element code (PRONTO – 3D) for the study of deformation of projectile and for overall damage [30], where an analytical force function derived from the dynamic cavity expansion theory was used to represent the target and the projectile was simulated by an explicit FE code PRONTO – 3D. This methodology avoids the target discretization, contact algorithms, and verified for metallic and geo – material targets [3, 31 – 33].

Analytical models based on the penetration resistance formulation are efficient, accurate, and capable of predicting the penetration depth into various targets. The dynamics of the projectile motion during penetration can be determined analytically and the nose geometry of the projectile can be included in the model. Since the interactions between the projectile and the target occur on the surface of the projectile, the DAFL method greatly extended the capability of the analytical model into more general simulations of projectile trajectory and deformation.

**Analytical Multi – Stage models for Perforation:** Corbett et al. [34], introduced a multi – stage models, firstly applied for metallic targets. Later on yankelevsky [35] proposed Two – stage model for perforation of concrete targets against the impact of hard missile under low velocities. The first stage is dynamic penetration, where

a disk model developed to calculate the stress field and the penetration resistance in front of the projectile nose. The second stage is plug formation and the shear – out of the plug. And during transition phase from first stage to second stage, the total penetration resistance in front of the projectile nose equals to shear resisting force offered by the remaining thickness of the target [36].
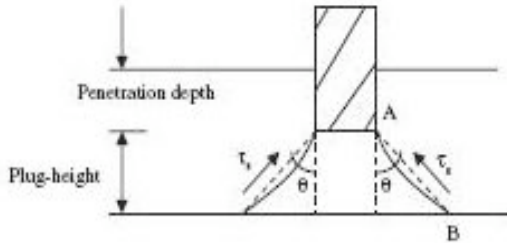
$$F_R = {}_f A_s \cos ( ) \qquad (17)$$



Fig.2. Shows a multi-stage perforation model.

Where   is cone slope angle, and $A_s$ is the surface area of cone plug. The two stage mechanism agrees with experimental observations that there are clear distinctions between the penetration and plugging processes. Li and Tong [36] combined the shear plug model with the penetration model for cratering and penetration to formulate the perforation of the concrete target. The normalized perforation limit (e) can be determined by:

$$e/d = H/d + x/d \qquad (18)$$

Where non-dimensional plug thickness H/d is:

$$\frac{H}{d} = \frac{1}{2\tan(\alpha)}$$

$$\left( \sqrt{1 + 2S \tan(\alpha)\left( \frac{3I(1 + (I/N))}{\pi tk(1 + (\pi tk/4N))} \right)^{1/2}} - 1 \right) \qquad (19)$$

$$x/d \le k, \text{ and}$$

$$\frac{H}{d} = \frac{1}{2\tan(\alpha)}\left( \sqrt{1 + \sqrt{3}S\tan(\alpha)} - 1 \right) \text{ for } x/d > k. \qquad (20)$$

A two-stage model was also recommended by the UKAEA [40] for through-thickness cone cracking. The impact velocity to initiate through-thickness cone cracking, $V_{cc}$, may be estimated by the following equations:

$$V_{cc} = 9.4 \times 10^{-2} \sqrt{f_c}\left( \frac{dH_o^2}{M} + \frac{H_o^3}{M} \right)^{1/2} \text{ for } 0.5 < H_o/d \le 1.82 \qquad (21)$$

And

$$V_{cc} = 0.117\sqrt{f_c}\left( H_o^3 / M \right)^{1/2} \text{ for } 1.82 < H_o/d < 4 \qquad (22)$$
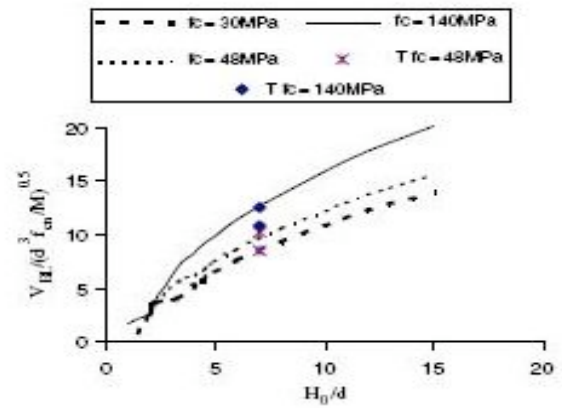


Fig.3. Shows the graphical representation of $H_o/d$ against eq. (22). Which were validated for $26 < f_c < 35$ (MPa), $24,000 < M/(d^2 H_0) < 1.5 \times 10^6$ (kg/m$^3$) and $2 < V_{cc} < 4.5$ (m/s). In the range $1.82 < H_0/d < 4$, penetration and then a cone crack were produced at the cone cracking velocity, ($V_{cc}$). For $0.5 < H_0/d \le 1.82$, cone cracking occurred from the beginning and was not preceded by penetration. Multi-stage models have not considered possible scabbing on the distal surface of the target. Experimental results and empirical formulae support the contention that the scabbing limit is generally greater than the perforation limit, i.e. $h_s > e$. This indicates three possibilities: (a) if $H_0 > h_s$, both scabbing and perforation do not occur, (b) if $h_s > H_0 > e$, scabbing occurs without perforation and (c) if $h_s > e > H_0$, both scabbing and perforation occur. Because scabbing removes material from the distal side of the target, it could play an important role in the initiations of both perforation and cone cracking. This issue should be further investigated.

### III. ANALYTICAL MODEL FOR PENETRATION DEPTH (X) AND PERFORATION LIMIT (E) OF REINFORCED CONCRETE TARGET

**Model for Penetration depth (x):** X.W. Chen and X.L. Li suggested an analytical model for penetration depth (x) and for perforation limit (e) of reinforced concrete target. The limitation of that model is projectile impact on concrete target on perpendicular direction, based on dynamic cavity expansion theory normal penetration in concrete target the initial crater is assumed as a cone with axial depth (kd) where k is non-dimensional parameter equals to 0.707 + h/d as given in Li and Chen [15]. For thick concrete targets the axial resistance forces on the projectile nose during the initial cratering and penetration processes:
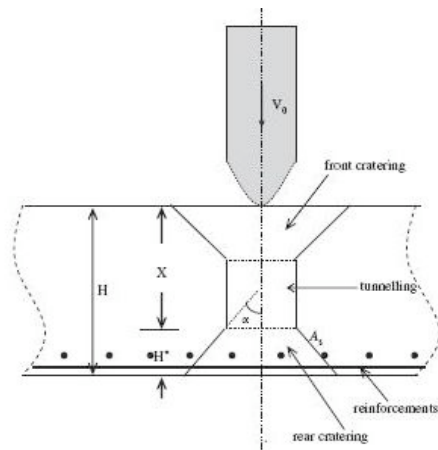


Fig.4. Shows normal penetration and perforation of thick reinforced concrete targets.

170

$$F_R = cx \qquad \text{for } x < kd \qquad (23)$$

$$Fr = \frac{\pi d^2}{4}\left(S f_c + N^* \ell V^2\right) \qquad \text{for } x \geq kd \qquad (24)$$

Where S is an empirical constant related to unconfined compressive strength of concrete $f_c$, c is experimental constant, x is the instantaneous penetration depth, and is density of concrete target. S can be calculated by [15,16]:

$$S = 82.6\, f_c^{-0.544}, \qquad \text{or} \qquad (25)$$

$$S = 72\, f_c^{-0.5} \qquad (f_c \text{ in MPa})[15,16] \qquad (26)$$

Impact function (I), Geometry function (N), and Nose function (N*) are:

$$I = \frac{MV_o^2}{d^3 S f_c}, \qquad N = \frac{M}{\ell d^3 N^*} \qquad (27), \text{ and } (28)$$

And

$$N^* = \frac{8}{d^2}\int_0^h \frac{yy'^3}{1 + y'^2}dx \qquad (29)$$

Where y is geometric definition of projectile nose curve, according to Li and Chen [19] and Chen et al. [49], the dimensionless maximum penetration depth for semi-infinite concrete target can be calculated by using:

$$\frac{X}{d} = \sqrt{\frac{\left(4k/\pi\right)\left(1 + k\pi/4N\right)}{\left(1/I + 1/N\right)}} \quad \text{for } x/d \leq k \qquad (30)$$

$$\frac{X}{d} = \frac{2}{\pi} N \ln\left[\frac{\left(1 + I/N\right)}{1 + k\pi/4N}\right] + k. \quad \text{for } x/d > k \qquad (31)$$

Here the dimensionless penetration depth measured in stages of initial cratering and tunneling is X/d = x(1 − H* / H). The final penetration depth without perforation can be obtained easily by substituting I = 0 and considering that no final plugging failure occurs:

$$x\left(1 - \frac{H^*}{H}\right) = \sqrt{\frac{\left(4k/\pi\right)\left(1 + \pi k/4N\right)}{\left(1/I + 1/N\right)}}$$

$$-\sqrt{\frac{\left(4k/\pi\right)\left(1 + \pi k/4N\right)}{\left(1/I_* + 1/N\right)}} \quad \text{for } x/d \leq k \qquad (32)$$

When N » I, and N » 1, which is associated with sharp and slender projectiles, the final penetration depth can be simplified as:

$$\frac{X}{d} = \sqrt{\frac{4k}{\pi}}\, I, \quad \text{for } x/d \leq k \text{ or } I \leq \frac{\pi k}{4} \qquad (33)$$

$$\frac{X}{d} = \frac{2I}{\pi} + \frac{k}{2}, \quad \text{for } x/d > k \text{ or } I > \frac{\pi k}{4} \qquad (34)$$

**Model for Perforation limit (e):** The model for perforation limit of reinforced concrete target against hard missile suggested by X.W. Chen and X.L. Li based on shear plugging criteria. The formation of plug is related with shear failure of target, at normal impact plug considered as cone shape with the cone shape angle ( ), = 60° [35, 37, and 50] for normal plain concrete, however because of reinforcement, in reinforced concrete the residual height of cone shaped plug may become thinner and cone slope angle ( ) may become increase also. In this model X.W. Chen and X.L. Li assumed a general cone slope angle ( ) for formulation, $A_s$ is the cone shaped plug, and H* is cone-shaped plug or residual thickness of the rear crater. In the case of normal perforation, the shear area of the conical plug surface is:

$$A_s = \frac{\pi x d^2}{Cos\alpha}\frac{H^*}{H}\left(1 + x\frac{H^*}{H}\tan\alpha\right), \qquad (35)$$
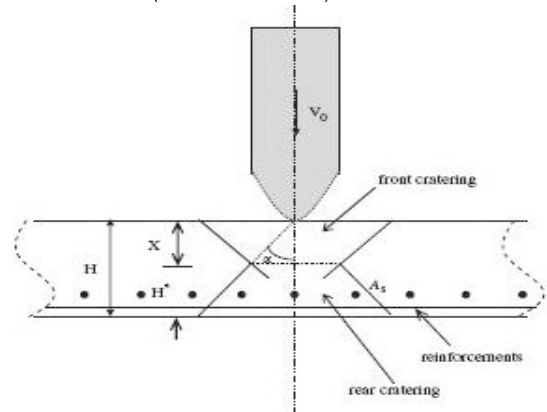
Fig.5. Shows normal penetration and perforation of thin reinforced concrete targets.

In plain concrete it is assumed that the plug is separated from surrounding of concrete as soon as the shear failure criteria satisfied along the plug surface. The failure stress in pure shear ( f) is equal to (3^-0.5 fc). In reinforced concrete target the tensile failure of reinforcement should be considered during the separation of rear plug from the target.
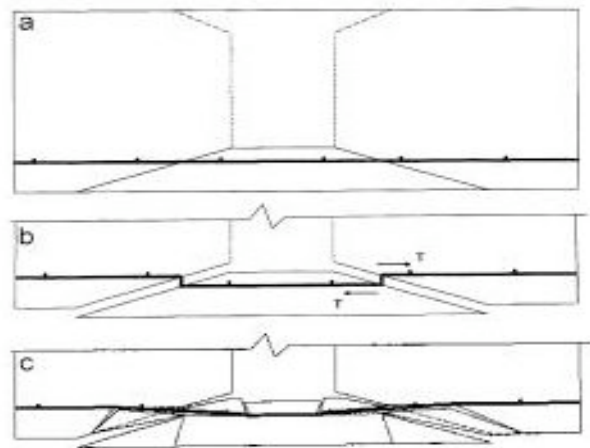
Fig.6(a),(b),(c). Shows the schematic description of the failure process at rear face of reinforced concrete targets.

In reinforced concrete targets may be some other case exists rear crater may be occurs in concrete without reaching tensile yield in reinforced bars. In this case projectile may be unable to perforate

171

the reinforced concrete target resisted by reinforcement. Thus the failure criteria defined in two phases: Shear failure of concrete and tensile failure of reinforced bars, and shear plugging occurs as soon as the resistant force ahead of the projectile nose reaches a critical value:

$$F = \frac{1}{\sqrt{3}} f_c A_s Cos\alpha + 2\pi H R_d \ell_s f_s Sin\alpha, \qquad (36)$$

Here the right hand side of above equation is equal to force component in the motion direction derived from the total shear plug surface, and the sin in second term gives assumption about the reinforcement bar is normal to the conical plug surface after rotating an angle at the moment of plugging failure. $R_d$ is the radius of cross-section or rear plug in which the layout of reinforcement bars is located, it is assumed to be the middle cross section of the plug, $R_d$ can be calculated by:

$$R_d = (d/2) + \left(H^*/2\right)\tan\alpha \qquad (37)$$

Besides considering the three dominant dimensionless numbers in the perforation of concrete slabs, i.e., the impact function I, the geometry function of projectile N and the dimensionless thickness of concrete panel x, reinforcement ratio $\rho_s$ of concrete and the uni-axial tensile strength $f_s$ of reinforcing steel bars are considered as the other main factors influencing the perforation process. In general, $f_s$ represent material property of reinforcing bars, and $\rho_s$ generally depicts the geometric character of reinforcing meshes, which includes the mesh size, space and diameter of reinforcing bars, etc. Therein a dimensionless number is introduced, which is simultaneously related to the reinforcement ratio $\rho_s$ and the uni-axial tensile strength $f_s$ of reinforcing bars.

$$\Theta = \sqrt{3x\ell_s f_s / f_c}\, Sin\alpha \qquad (38)$$

$$\frac{H^*_{BL}}{d} = \frac{\sqrt{\left(1 + \sqrt{3}\,S/4k + \Theta \tan\alpha\right)^2 + \left(\sqrt{3}Sx/k - 4\Theta\right)\tan\alpha}}{2\tan\alpha} \qquad (39)$$

$$- \frac{\left(1 + \sqrt{3}\,S/4k + \Theta \tan\alpha\right)}{2\tan\alpha}, \quad \text{for } X/d \leq k.$$

$$F = \frac{1}{\sqrt{3}} f_c A_s Cos\alpha\left(1 + \Theta\frac{d}{H^*}\right) \qquad (40)$$

In which $\Theta = 0$ represents the case of plain concrete.

$$A_s Cos\alpha\left(1 + \Theta\frac{d}{H^*}\right) = \frac{\sqrt{3}\pi d^2 Sx}{4k}\left(1 - \frac{H^*}{H}\right), \text{ for } x/d \leq k \qquad (41)$$

$$A_s Cos\alpha\left(1 + \Theta\frac{d}{H^*}\right) = \frac{\sqrt{3}\pi d^2 Sx}{4k}, \text{ for } x/d > k \qquad (42)$$

Obviously, $A_s$ and $H^*/H$ are independent of initial impact velocity $V_o$ and can be determined by the geometric configuration of perforation. It is only induced from the assumption of N » I and N » 1 and a more general conclusion cannot be achieved.

IV.     ANALYTICAL MODEL FOR PENETRATION DEPTH (X) AND PERFORATION LIMIT (E) AT OBLIQUE BY RIGID MISSILE ON CONCRETE TARGET

Consider a model similar to Recht and Ipson [51], and Ipson and Recht [52], with assumption of angular direction ( ) take place near the front surface in the process of initial cratering due to action of

asymmetric resistance. Therefore the thickness of target at angle considered as effective thickness of target and it is equal to $H_{eff} = H / Cos( + )$. According to Forrestal et al. [16, 53], Li and Chen [15, 54] based on dynamic cavity expansion theory there is only drag force along the axial direction of projectile after projectile head entering the concrete target.
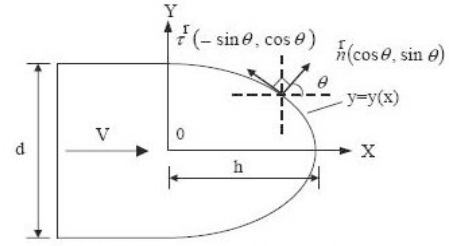


Fig.7. Shows the details of contact point of nose shape missile at oblique concrete target.

It is known that the impact damage of a concrete target subjected to the normal impact of a rigid projectile consists of a conical crater with depth (kd) and a tunnel with the size of the projectile shank diameter (d), based on slip-line theory Li and Chen [15, 54] suggested k = (0.707 + h/d) for normal impact of hard missile on concrete. Similarly, for oblique penetration, the initial crater is assumed as an oblique-crossed cone with an axial depth kd, where k = (0.707 + h/d)Cos .
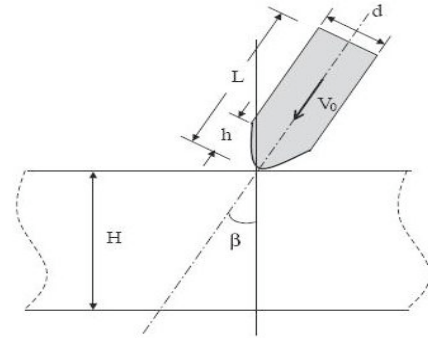


Fig.9. Shows the penetration and perforation model of concrete target by a rigid projectile at initial obliquity angle .
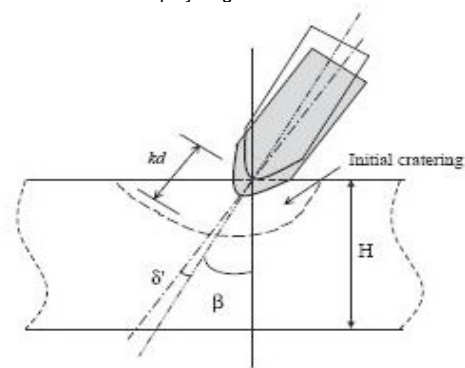


Fig.10. Shows the first stage of impact Directional change of projectile.

Recht and Ipson [51] and Ipson and Recht [52] approximately defined an angular directional change d by considering the impulse component transferred to the panel target. Basically, the component of the initial momentum normal to the submerging path is transferred to the target; only the momentum in the direction defined by  will be active in the perforation process. Nevertheless, their models cannot evaluate quantitatively the effect of projectile geometry, target material and impact velocity, etc. Later on, The X.W. Chen, S.C. Fan, and Q.M. Li [49] assumed a model by using

the kinetic energy consumption normal to the submerging path to calculate the angle of directional change . The component of impact velocity normal to the submerging path is:

$$V = V_o Sin \qquad (43)$$

The curved path of directional change is s, which can approximately consider as an arc:

$$s_\perp = x\delta, \qquad \text{for x/d} \le k \qquad (44)$$

$$s_\perp = \delta k d, \qquad \text{for x/d} > k \qquad (45)$$

In [55] experimental results show that the resistant drag increases almost linearly with time in the first stage, so the average lateral force is:

$$F_{\perp avg} = \frac{1}{2} F_o Sin\beta = \frac{1}{2}\frac{cx}{d}Sin\beta, \quad \text{for x/d} \le k, \qquad (46)$$

$$F_{\perp avg} = \frac{1}{2} F_o Sin\beta = \frac{1}{2}\frac{\pi d^2}{4}\left(Sf_c + N^*\ell V_o^2\right)in\beta, \quad \text{for x/d} > k, \qquad (47)$$

$$\text{Where } F_o = c(x/d) \qquad \text{for (x/d)} \le k \qquad (48)$$

$$Fr = \frac{\pi d^2}{4}\left(Sf_c + N^*\ell V^2\right) \qquad \text{for } x \ge kd \qquad (49)$$

The kinetic energy consumption normal to submerging path, and the angle of directional changes respectively:

$$\frac{1}{2}MV_\perp^2 = F_{\perp avg} S_\perp \qquad (50)$$

And

$$Sin^2\delta = \delta Sin\beta\left(\frac{1}{I} + \frac{1}{N}\right)$$

$$\left(\frac{1}{\sqrt{\left(\frac{1}{ICos^2\delta}\right)+1/N}} - \frac{1}{\sqrt{\left(\frac{1}{I_*}\right)+1/N}}\right)^2, \text{ for } \frac{x}{d} \le k \qquad (51)$$

$$Sin^2\delta = \delta Sin\beta \frac{\pi k}{4}\left(\frac{1}{I} + \frac{1}{N}\right), \text{ for } \frac{x}{d} > k \qquad (52)$$

Where

$$I_* = MV_*^2 \Big/ Sf_c d^3 \qquad (53)$$

By Li and Chen [15, 54] and Chen and Li [19], for sharper nose and slender shrank projectiles in many practical cases N » I, particularly N » 1. As I > I*, for smaller directional change ( 0) :

$$\delta = Sin\beta\left(- \sqrt{I_*/I}\right) \text{ for } \frac{x}{d} \le k \qquad (54)$$

$$\delta = \frac{\pi k Sin\beta}{4I}, \quad \text{for x/d} > k \qquad (55)$$

The above equations give the quantitative demonstration on the effects of projectile geometry, target material, impact velocity and initial obliquity on the angle of direction change.
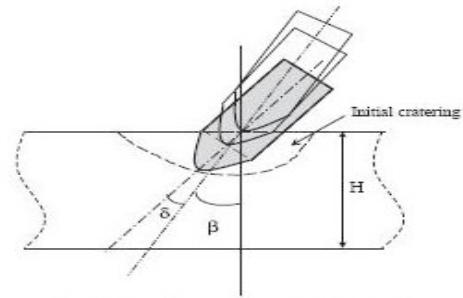


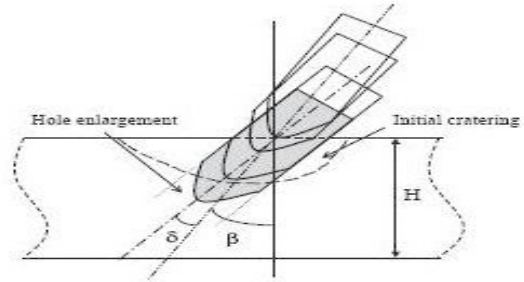Fig.11. Shows the end of first stage (Initial cratering).



Fig.12. Shows the tunneling process after dimensional change.

After the initial cratering stage of directional change, the projectile penetrates into target along X direction at an angle of ( + ) purely followed the dynamic cavity expansion theory. The motion of the rigid projectile is governed by Newton's second law of motion together with initial conditions of V(t = 0) = V₀Cos and X(t=0) = 0, can be integrated to obtain the final penetration depth [15, 54]:

$$\frac{X}{d} = \sqrt{\frac{(4k/\pi)(1+\pi k/4N)}{\left(\sqrt{I\cos^2\delta}+1/N\right)}} \quad \text{for } \frac{X}{d} \le k \text{ or } I\cos^2\delta \le \frac{\pi k}{4} \qquad (56)$$

And

$$\frac{X}{d} = \frac{2}{\pi}N\ln\left[\frac{1+I\cos^2\delta/N}{1+\pi k/4N}\right] + k, \text{ for } \frac{X}{d} > k \text{ or } I\cos^2\delta > \frac{\pi k}{4} \qquad (57)$$

For N » I and N » 1

$$\frac{X}{d} = \sqrt{\frac{4k}{\pi}I\cos^2\delta}, \quad \text{for } \frac{X}{d} \le k \quad \text{or } I\cos^2\delta \le \frac{\pi k}{4} \qquad (58)$$

and

$$\frac{X}{d} = \frac{2I\cos^2\delta}{\pi} + \frac{k}{2} \quad \text{for } \frac{X}{d} > k \quad \text{or } I\cos^2\delta > \frac{\pi k}{4} \qquad (59)$$

The above equation can be used to predict the penetration depth of hard missile into the thick concrete structures at oblique impact.

**Oblique Perforation model of concrete targets:** Perforation occurs after the process of penetration when a plug is formed between the projectile nose and the rear face of the concrete target.
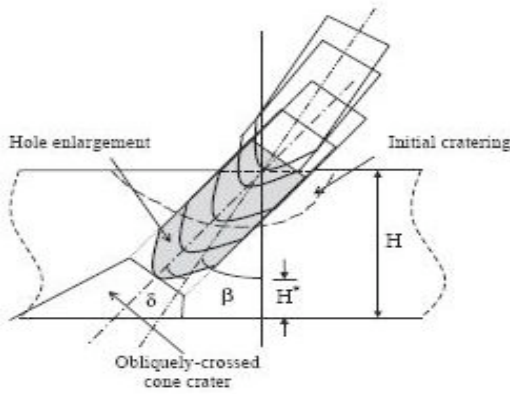
173

Fig.13. Shows initiation of rear cratering.

For oblique impact as similar to normal impact only with the change of plug is idealized as an oblique crossed cone having same cone slope angle as in normal impact with the oblique crossed angle ($\beta + \delta$)
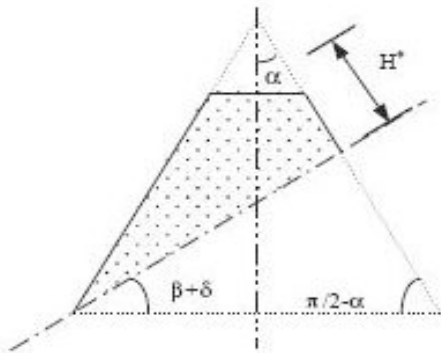


Fig.14. Shows the geometric sketch of rear, oblique crossed cone crater.

The failure stress in pure shear $\tau_f = 3^{-0.5}f_c$, as concrete is brittle material having low tensile strength approximately equal to 10% of the compressive strength, because of this reason plug is separated from the surrounding material as soon as shear failure criterion satisfied along the plug surface. The disintegration is caused by the tensile stresses arising from the complicated reflections of stress wave prior to shear plugging. It is assumed that $A_s$ is the shear surface area of the oblique crossed cone plug, and $H^*$ is the residual thickness of the oblique crossed cone plug, i.e., the normal distance between the rear face and the nose tip. $A_s$ and $H^*$ are the functions of , , and , which can be determined by simple geometrical relations.
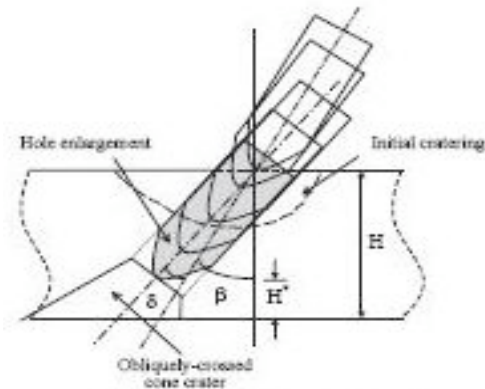


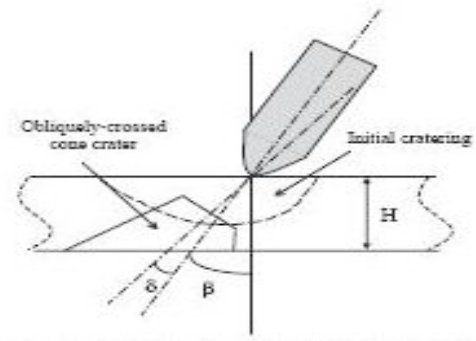Fig.15. Shows the Initiation of rear cratering (with tunneling process).



Fig.16. Shows the oblique perforation of thin concrete target (no tunneling process).

There're two scenarios for perforation:
a. Initial cratering immediately followed by shear plugging ($x/d \leq k$), no hole enlargement, and
b. Complete perforation ($x/d > k$), in which penetration process is also included.

The dimensionless penetration depth measured along the oblique angle ($\beta + \delta$) in the stages of initial cratering and tunneling in $x/d = (H - H^*) \sec(\beta + \delta) / d$. For different scenarios of perforation, it can be formulated:

$$x \sec(\beta + \delta)\left(1 - \frac{H^*}{H}\right) = \sqrt{\frac{\left(4k/\pi\right)\left(1 + \pi k/4N\right)}{\left(\left(I \cos^2 \delta\right) + \left(1/N\right)\right)}}$$

$$- \sqrt{\frac{\left(4k/\pi\right)\left(1 + \pi k/4N\right)}{\left(1/I_*\right) + 1/N}}, \quad \text{for } \frac{x}{d} \leq k \tag{60}$$

$$x \sec(\beta + \delta)\left(1 - \frac{H^*}{H}\right) = \frac{2}{\pi} N \ln\left[\frac{N + I \cos^2 \delta}{\left(1 + \pi k/4N\right)\left(N + I_*\right)}\right] + k, \quad \text{for } \frac{x}{d} > k \tag{61}$$

Where $x = H/d$ is the dimensionless thickness of concrete target. Since concrete is brittle material, shear plugging occurs as soon as the resistance force ahead of the projectile nose reaches a critical value:

$$F = \frac{1}{\sqrt{3}} f_c A_s \cos\alpha, \tag{62}$$

Where right hand side of above equation is the force component in the motion direction derived from the total shear plug surface,

$$\frac{f_c A_s \cos\alpha \cos(\beta + \delta)}{\sqrt{3}cx} = \left(1 - \frac{H^*}{H}\right), \quad \text{for } \frac{x}{d} \leq k \tag{63}$$

$$\frac{1}{\sqrt{3}} f_c A_s \cos\alpha = \frac{\pi d^2}{4}\left(Sf_c + N^* \ell V_*^2\right) \quad \text{for } \frac{x}{d} . k \tag{64}$$

$$\left(1 + \frac{\pi k}{4N}\right)\exp\left[\frac{\pi x \sec(\beta + \delta)}{2N}\left(1 - \frac{H^*}{H}\right) - \frac{\pi k}{2N}\right]$$

$$= \frac{\sqrt{3}\pi S d^2}{4 A_s \cos\alpha}\left(1 + \frac{I \cos^2 \delta}{N}\right). \tag{65}$$

According to the definitions of c, , and $A_s$, above equations manifest the dependence of $H^*/H$ on the initial velocity $V_o$ and the geometric configuration in both cases ($x/d \leq k$ and $x/d > k$). If $N \gg I$ and $N \gg 1$ then:

174

$$A_S \cos \alpha = \frac{\sqrt{3}\pi d^2 Sx}{4k \cos(\beta + \delta)} \left(1 - \frac{H^*}{H}\right), \quad \text{for } \frac{x}{d} \le k, \quad (66)$$

$$A_S \cos \alpha = \frac{\sqrt{3}\pi d^2 S}{4}, \quad \text{for } \frac{x}{d} > k, \quad (67)$$

Furthermore, if I is large enough (I > 10 or $V_o$ > 500m/s), the angular directional change is negligible regardless of the target thickness. Besides, $A_s$ and $H^*/H$ are independent of initial impact velocity $V_o$ and can be determined by the geometric configuration of perforation.

To achieve perforation, a projectile having slender shank and sharp nose (e.g., ogive or conical shapes) is frequently used. It corresponds to a larger value of the geometry function N(N ~ 200) see [15, 54]. For the cases of N » 1, which are the common cases in practice, much simpler formulae can be deduced.

## V. CONCLUSIONS

In this paper the local impact effects of a hard projectile on concrete targets have been discussed. The paper consists of analytical concept studies on local impact phenomenon.
Analytical model on penetration depth, perforation and scabbing limits, as well as their ranges of application.

## VI. REFERENCES

[1] Kennedy RP. A review of procedures for the analysis and design of concrete structures to resist missile impacteffects. Nucl. Eng. Des 1976;37:183–203.
[2] Li QM, Reid SR, Wen HM, Telford AR. Local impact effects of hard missiles on concrete targets. Int J Impact Eng 2005;32(1–4):224–84.
[3] Warren TL, Poormon KL. Penetration of 6061-T6511 aluminum targets by ogive-nosed VAR 4340 steel projectiles at oblique angles: experiments and simulations. Int J Impact Eng 2001;25:993–1022.
[4] Allen WA, Mayfield EB, Morrison HL. Dynamics of a projectile penetrating sand. J Appl Phys 1957;28(3):370–6.
[5] Forrestal MJ, Tzou DY. A spherical cavity-expansion penetration model for concrete targets. Int J Solids Struct. 1997;34(31–32):4127–46.
[6] Forrestal MJ, Frew DJ, Hickerson JP, Rohwer TA. Penetration of concrete targets with deceleration-time measurements. Int J Impact Eng 2003;28:479–97.
[7] Wen HM. Penetration and perforation of thick FRP laminates. Compos Sci Technol 2001;61:1163–72.
[8] Wen HM. Predicting the penetration and perforation of targets struck by projectiles at normal incidence. Mech. Struct. Mach 2002;30(4):543–77.
[9] Bishop RF, Hill R, Mott NF. The theory of indentation and hardness tests. Proc Phys Soc 1945;57(Part 3):147–59.
[10] Hill R. A theory of earth movement near a deep underground explosion. Memo No. 21–48, Armament Research Establishment, Front Halstead, Kent, UK, 1948.
[11] Hopkins HG. Dynamic expansion of spherical cavities in metals. In: Sneddon IN, Hill R, editors. Progress in solid mechanics, vol. 1. Amsterdam, New York: North-Holland; 1960 Chapter 3.
[12] Goodier JN. On the mechanics of indentation and cratering in solid targets of strain-hardening metal by impact of hard and soft spheres. AIAA proceedings of the seventh symposium on hypervelocity impact III, 1965. p. 215–59.
[13] Forrestal MJ, Luk VK. Penetration into soil targets. Int J Impact Eng 1992;12:427–44.
[14] Forrestal MJ, Tzou DY, Askari E, Longcope DB. Penetration into ductile metal targets with rigid spherical-nose rods. Int J Impact Eng 1995;16:699–710.
[15] Li QM, Chen XW. Dimensionless formulae for penetration depth of concrete target impacted by a nondeformable projectile. Int J Impact Eng 2003;28(1):93–116.
[16] Forrestal MJ, Altman BS, Cargile JD, Hanchak SJ. An empirical equation for penetration depth of ogive-nose projectiles into concrete targets. Int J Impact Eng 1994;15(4):395–405.
[17] Forrestal MJ, Luk VK. Dynamic spherical cavity expansion in a compressible elastic–plastic solid. J Appl Mech ASME 1988;55:275–9.
[18] Luk VK, Forrestal MJ, Amos DE. Dynamics spherical cavity expansion of strain-hardening materials. ASME J Appl Mech 1991;58(1):1–6.
[19] Chen XW, Li QM. Deep penetration of a non-deformable projectile with different geometrical characteristics. Int J Impact Eng 2002;27:619–37.
[20] Xu Y, Keer LM, Luk VK. Elastic-cracked model for penetration into unreinforced concrete targets with ogival nose projectiles. Int J Solids Struct 1997;34(12):1479–91.
[21] Durban D, Masri R. Dynamic spherical cavity expansion in a pressure sensitive elastoplastic medium. Int J Solids Struct 2004;41:5697–716.
[22] Murff JD, Coyle HM. Low velocity penetration of Kaolin. ASCE J Soil Mech Found Div 1973;99(SM5):375–89.
[23] NDRC. Effects of impact and explosion. Summary Technical Report of Division 2, vol. 1, National Defence Research Committee, Washington, DC, 1946.
[24] Riera JD. Penetration, scabbing and perforation of concrete structure hit by solid missile. Nucl Eng Des 1989;115:121–31.
[25] Haldar A, Hamieh H. Local effect of solid missiles on concrete structures. ASCE J Struct Div. 1984;110(5):948–60.
[26] Heuze FE. Overview of projectile penetration into geological materials, with emphasis on rocks. Int J Rock Mech Min Sci Geomech Abstr 1990;27(1):1–14.
[27] Greighton DC. Non-normal penetration in soil and rock: user's guide for computer code PENCO2D. US Army Waterways Experiment Station, Vicksburg, Technical Report SL-82-7, 1982.
[28] Adley MD, Berger RP, Cargile JD, White HG, Greighton DC. Three dimensional projectile penetration into curvilinear geological/structural target. User's Guide for PENCRV3D, US Army Waterways Experiment Station, Instruction Report SL-97-1, Vicksbury, M.S., January 1997.
[29] Danielson KT, Adley MD. A meshless treatment of three-dimensional penetrator targets for parallel computation. Comput Mech 2000;25:267–73.
[30] Warren TL, Tabbara MR. Spherical cavity-expansion forcing function in PRONTO 3D for applications to penetration problems, SAND97-1174. Albuquerque, NM: Sandia National Laboratories; 1997.
[31] Warren TL, Tabbara MR. Simulations of the penetration of 6061-T6511 aluminum targets by spherical-nosed VAR 4340 steel projectiles. Int J Solids Struct 2000;37(3/2):4419–35.
[32] Warren TL. Simulations of the penetration of limestone targets by ogive-nose 4340 steel projectile. Int J Impact Eng 2002;16:699–710.
[33] Warren TL, Fossum AF, Frew DJ. Penetration into low-strength (23 MPa) concrete: target characterization and simulation. Int J Impact Eng 2004;30:477–503.

[34] Corbett GG, Reid SR, Johnson W. Impact loading of plates and shells by free-flying projectiles: a review. Int J Impact Eng 1996;18:141–230.

[35] Yankelevsky DZ. Local response of concrete slabs to low velocity missile impact. Int J Impact Eng 1997;19(4):331–43.

[36] Li QM, Tong DJ. Perforation thickness and ballistic performance of concrete target subjected to rigid projectile impact. ASCE J Eng Mech 2003;129(9):1083–91.

[37] Dancygier AN. Rear face damage of normal and high-strength concrete elements caused by hard projectile impact. ACI Struct J 1998;95:291–304.

[38] Hanchak SJ, Forrestal MJ, Young ER, Ehrgott JQ. Perforation of concrete slabs with 48 and 140MPa unconfined compressive strength. Int J Impact Eng 1992;12(1):1–7.

[39] Sliter GE. Assessment of empirical concrete impact formulas. ASCE J Struct Div 1980;106(ST5):1023–45.

[40] Barr P. Guidelines for the design and assessment of concrete structures subjected to impact. Report, UK Atomic Energy Authority, Safety and Reliability Directorate, HMSO, London, 1990.

[41] Li QM, Reid SR. Development of concrete impact models. Report to Magnox Electric Ltd., Report Reference:MAME/AM/0304/4500288589/JKL, Department of Mechanical, Aerospace and Civil Engineering, UMIST, 2004.

[42] BNFL. Reinforced concrete slab local damage assessment. R3 impact assessment procedure, Appendix H, vol. 3. Magnox Electric plc & Nuclear Electric Limited; 2003.

[43] Chen XW, Li QM. Transition from non-deformable projectile penetration to semi-hydrodynamic penetration. ASCE J Mech Eng 2004;130(1):123–7.

[44] Forrestal MJ, Piekutowski AJ. Penetration experiments with 6061-T6511 aluminum targets and spherical-nose steel projectiles at striking velocities between 0.5 and 3.0 km/s. Int J Impact Eng 2000;24:57–67.

[45] Piekutowski AJ, Forrestal MJ, Poormon KL, Warren TL. Penetration of 6061-T6511 aluminum targets by ogivenose steel projectiles with striking velocities between 0.5 and 3.0 km/s. Int J Impact Eng 1999;23:723–34.

[46] Hazell PJ, Fellows NA, Hetherington JG. A note on the behind armour effects from perforated alumina/aluminium targets. Int J Impact Eng 1998;22:589–95.

[47] Rosenberg Z, Dekel E. Numerical study of the transition from rigid to eroding-rod penetration. J Phys IV Fr 2003;110:681–6.

[48] Li QM, Reid SR, Ahmad-Zaidi AM. Critical impact energies for scabbing and perforation of concrete target. Nucl Eng Des 2006;236:1140–8.

[49] Chen XW, Fan SC, Li QM. Oblique and normal penetration/perforation of concrete target by rigid projectiles. Int J Impact Eng 2004;30(6):617–37.

[50] Dancygier AN, Yankelevsky DZ. High strength concrete response to hard projectile impact. Int J Impact Eng 1996;18(6):583–99.

[51] Recht RF, Ipson TW. Ballistic perforation dynamics. J Appl Mech -Trans ASME 1963;30:385–91.

[52] Ipson TW, Recht RF. Ballistic penetration resistance and its measurement. Exp Mech 1975;15:249–57.

[53] Forrestal MJ, Frew DJ, Hanchak SJ, Brar NS. Penetration of grout and concrete targets with ogive-nose steel projectiles. Int J Impact Eng 1996;18(5):465–76.

[54] Li QM, Chen XW. Penetration into concrete targets by a hard projectile. Structures under shock and impact VII. In: JonesN, Brebbia CA, Rajendran AM, editors. Seventh International Conference on Structures under Shock and Impact (SUSI/7). May 27–29, Montreal, Southampton: WIT Press; 2002. p. 91–100.

[55] Buzaud E, Laurensou R, Darrigade A, Belouet P, Lissayou C. Hard target defeat: an analysis of reinforced concrete perforation process. The 9th International Symposium on Interaction of the Effects of Munitions with Structures, Berlin, Germany; 3–7 May, 1999, pp. 283–290.